

Introduction

- Einstein-Newcomb-de-Sitter (ENdS) space (Fig.1) is a modification of the Einstein space made by de Sitter [1] a few months after Einstein published his first cosmological model [2] in 1917. De Sitter used Newcomb's elliptical space [3] and found that, similarly to the Einstein space, it equally satisfies Einstein's field equations.
- This is a static space with its antipodal points topologically identified (Fig.2). The topological identification of antipodal points is a mathematical abstraction. This can be interpreted physically as a connection between remote points via the Einstein-Rosen bridge (Fig.3), also called "wormhole".
- Distances are measured by the projective angle χ , such that the distance along the spherical "surface" is $r' = R\chi$ (Fig.1). The maximal distance in Einstein's spherical space corresponds to $\chi = \pi$, whereas in elliptical space it is $\chi = \pi/2$, as the points separated by $\chi = \pi$ correspond to the same point in elliptical space.

Fig.1: Embedding diagram depicting elliptical space of constant positive curvature (the blue sphere) with two antipodal points topologically identified (the dark-blue connection between two poles) and with a tangential Euclidean space at the observer's location (o). Distances along the spatial coordinate (r') are measured by the projective angle χ ($r' = R\chi$), where R^{-2} is the curvature. The corresponding projective distance to the source (s) in the Euclidean space is $r = R \tan \chi$.

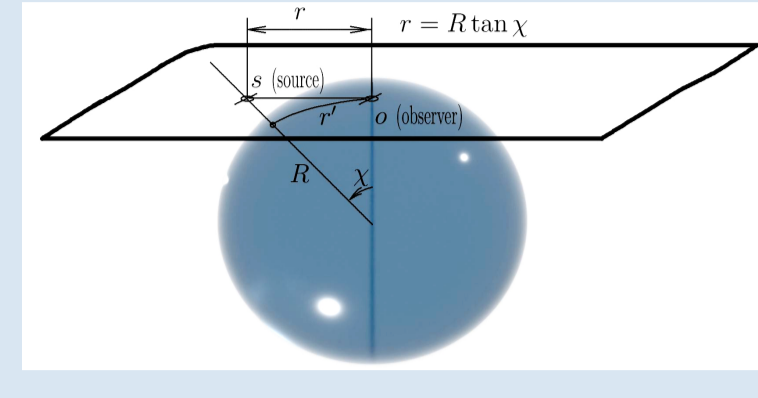


Fig.2: Simplified embedding diagram of elliptical space (curvature R^{-2} being ignored) highlighting the mathematical identification of two antipodal ($\chi = \pi$) points. The identification is indicated by the vertical dashed line connecting two points.

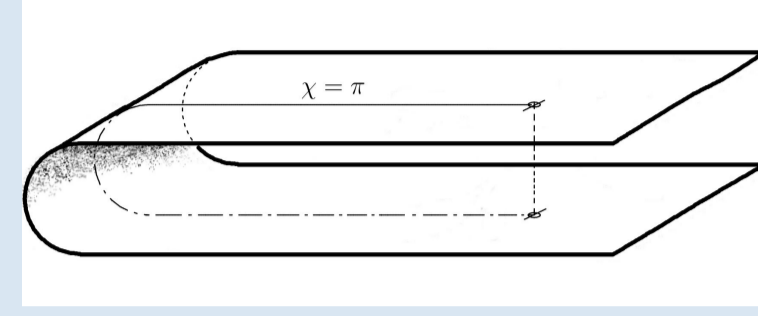
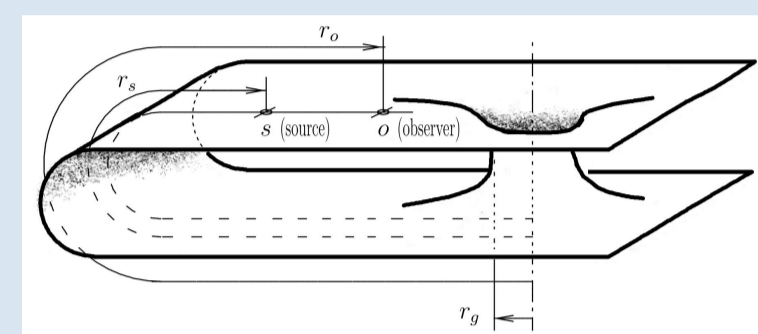


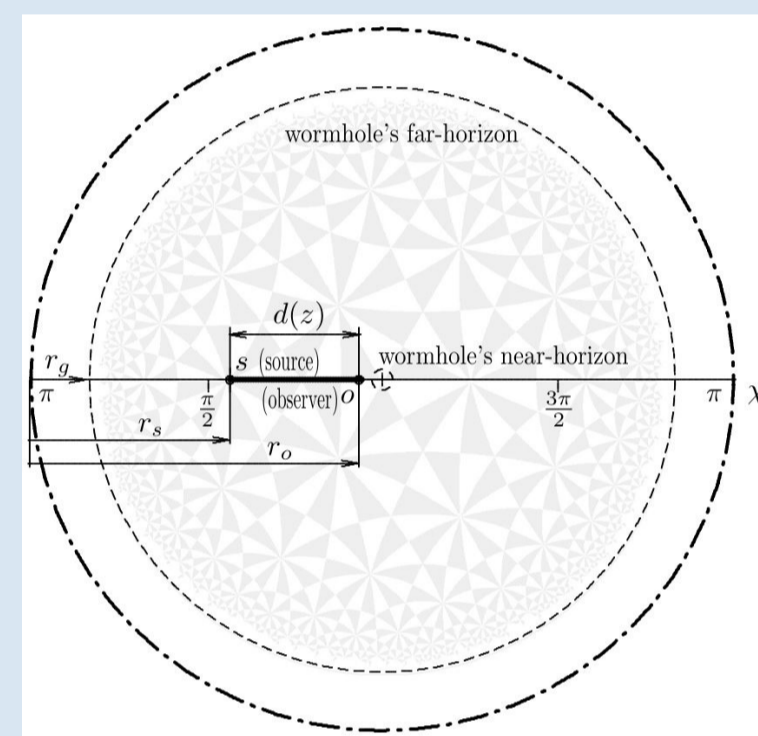
Fig.3: Embedding diagram depicting a possible physical realization of the topological connection between two distant (antipodal) regions of space via a wormhole structure. Here r_o and r_s are distances of the observer (o) and source (s) from the wormhole's far throat, opposite to the near throat in the vicinity of the observer, and r_g is the gravitational radius of the wormhole.



Distances in the ENdS space

- De Sitter's static cosmological model leads to the redshift-distance relationship which is discrepant with the observed standard-candles' relationship between luminosity distances and redshifts. This mismatch is due to de Sitter's overlook of the very aspect of elliptical space which he regarded as the most important aspect for modelling the physical world – namely, the topological identification of antipodal points. He completely neglected it and focused mainly on the differences between the local and remote coordinate systems (Fig.1) when relating distances to redshifts in his theory.
- But it is precisely this feature of identical antipodal points that allows relating the cosmological redshift with the time-dilatation effect inherent to the Schwarzschild solution of Einstein field equations. As with any Schwarzschild event horizon, there is an associated gravitational redshift, which is calculable when we know the distances from the horizon to the source and to the observer. Thus, in this particular setup, the observed cosmological redshift is gravitational by its nature.
- The Schwarzschild metric of the ENdS space leads to a distance-to-redshift relationship $d_L(z)$ (see formulae below Fig.4) which, in terms of accuracy, stays on equal footing with the distance-to-redshift relationship derived from the expanding-Universe cosmology based on the Λ CDM model.

Fig.4: Poincaré-map representation of distances in the ENdS space shown in Fig.3 above. They range from observer's point o ($\chi = 0$) to its antipodal point ($\chi = \pm\pi$). The dot-dashed circle in this map represents the observer's point o itself, but in the form of its antipodal image seen in all 4 directions from the observer. The smaller and larger dashed circles represent, respectively, the near- and far-event horizons of the wormhole. The distance of interest here is the source-to-observer distance $d = r_o - r_s$, which has to be expressed as a function $d(z)$ of source redshifts in order to compare the observed standard-candle (type Ia supernova) redshifts with their luminosity distances.



In this setup, we include unknown distances r_o , r_s , the source-to-observer distance $d = r_o - r_s$, and the unknown gravitational radius r_g . Both the source and observer are within the Schwarzschild metric, which corresponds to the following spacetime interval in spherical coordinates (r, θ, ϕ): $ds^2 = g_{tt}c^2 dt^2 - g_{rr} dr^2 - r^2(d\theta^2 + \sin^2\theta d\phi^2)$, where $g_{tt} = 1 - \frac{2a}{r}$ and $g_{rr} = \frac{1}{1 - \frac{2a}{r}}$. The source's redshift with respect to the observer is $z = \sqrt{g_{tt}(r_s)/g_{tt}(r_o)} - 1$, or, if we define $r_g = 1$ as the distance unit, $(1+z)^2 = (1 - \frac{2}{r_s}) / (1 - \frac{2}{r_o})$. Then the source-to-observer distance reads $d(z) = r_o - r_s = [1 - (1 - \frac{2}{r_o})(1+z)^{-2}]^{-1}$ [in units of r_g], which has to be multiplied by the scaling factor $(1+z)^2$ in order to obtain the luminosity distance $d_L(z) = \{r_o - [1 - (1 - \frac{2}{r_o})(1+z)^{-2}]^{-1}\} (1+z)^2$, with one of the $(1+z)$ factors accounting for the decrease in the number of incoming photons due to time dilatation in the Schwarzschild metric (the g_{tt} metric coefficient) and another accounting for the photon path distortion (the g_{rr} metric coefficient). This is the required redshift-luminosity relationship, permitting us to compare the ENdS-based model with observational data.

Comparison with observations

- In order to compare the theoretical luminosity distances with observational data (e.g., distance moduli of the type Ia supernovae), the distances need to be scaled and converted into magnitude values comparable with the observed source magnitudes.
- For our comparison, we use the well-calibrated sample of 1701 type Ia SNe, called "Pantheon+" [3,4]. The uncertainty of the parameters of the standard Λ CDM cosmological model were recently substantially reduced using this "Pantheon+" sample [5]. For example, the uncertainty in the H_0 parameter was reduced to ± 1 km/s/Mpc.
- Although the Λ CDM model was previously fitted to the "Pantheon+" sample, we repeat that fit here to ensure that our calculation algorithms, when applied to both Λ CDM and ENdS, remain the same, in order to consistently intercompare these two models.
- Starting with the Λ CDM model, the luminosity distance as a function of redshift, z is calculated in this model from $D_L(z) = D_A(z)(1+z)^2$, where the scaling factor $(1+z)^2$ is the same as in $d_L(z)$ equation of Fig.4, and D_A is the angular diameter distance: $D_A(z) = \frac{c}{H_0} \frac{1}{1+z} \int_0^z \frac{dz'}{\sqrt{1 + \Omega_M [(1+z')^3 - 1]}}$, as calculated for a flat cosmology ($\Omega_k = 0$). On the other hand, the luminosity distance is defined as the relationship between the bolometric flux and luminosity of a source, which is encoded in the source distance moduli provided by the "Pantheon+" sample.
- If D_L is expressed in Mpc, the distance modulus is $\mu_{\Lambda\text{CDM}} = 5 \log D_L + 25$. (1)

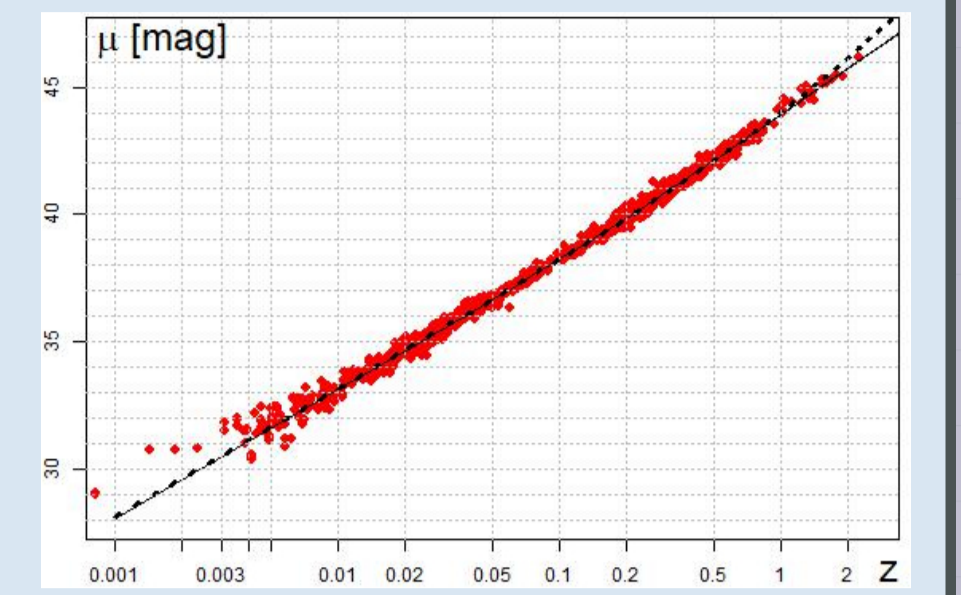
Estimation of Pearson's χ^2

- By fitting the theoretical values to the observationally determined distance moduli of type Ia supernovae we can find the values of the Λ CDM parameters. In the flat Λ CDM, there are two free parameters – H_0 and Ω_M – and a fixed parameter $\Omega_\Lambda = 1 - \Omega_M$. The fit can be achieved by minimising Pearson's χ^2 : $\chi^2 = \Delta D^T C^{-1} \Delta D$, where C is the covariance matrix and ΔD is the vector of SN distance-modulus residuals $\Delta D_i = \mu_{\Lambda\text{CDM}}(z_i) - \mu_i$, whose length is $N = 1701$ for the "Pantheon+" sample.
- Since here we are only interested in comparing the goodness of fit of two different cosmological models, we do not need to reach out for the correct cosmological parameters via these fits. Thus, we can use a simplified statistic $\chi^2 = (\text{diag } C^T \Delta D)^2 = \sum_{i=1}^N \frac{\Delta D_i^2}{\sigma_{\mu_i}^2}$, where $\sigma_{\mu_i}^2$ are the uncertainties of μ_i as determined from the diagonal of the covariance matrix

Fitting: Λ CDM

- For our comparison, we use μ_{SHOES} from [5], which are the corrected distance moduli where fiducial type Ia SNe magnitudes M were determined from SHOES 2022 Cepheid host absolute distances [6]. This minimisation of χ^2 gives $H_0 = 72.429^{+0.116}_{-0.109}$ [km/s/Mpc]; $\Omega_M = 0.389^{+0.010}_{-0.007}$, which differ, as expected, from those based on the full covariance matrix ($H_0 = 73.6 \pm 1.1$ [km/s/Mpc]; $\Omega_M = 0.334 \pm 0.018$ [5]). This is acceptable, as we are interested in the goodness of fit characterised by the minimal value $\chi^2_{\Lambda\text{CDM}} = 881.15$.

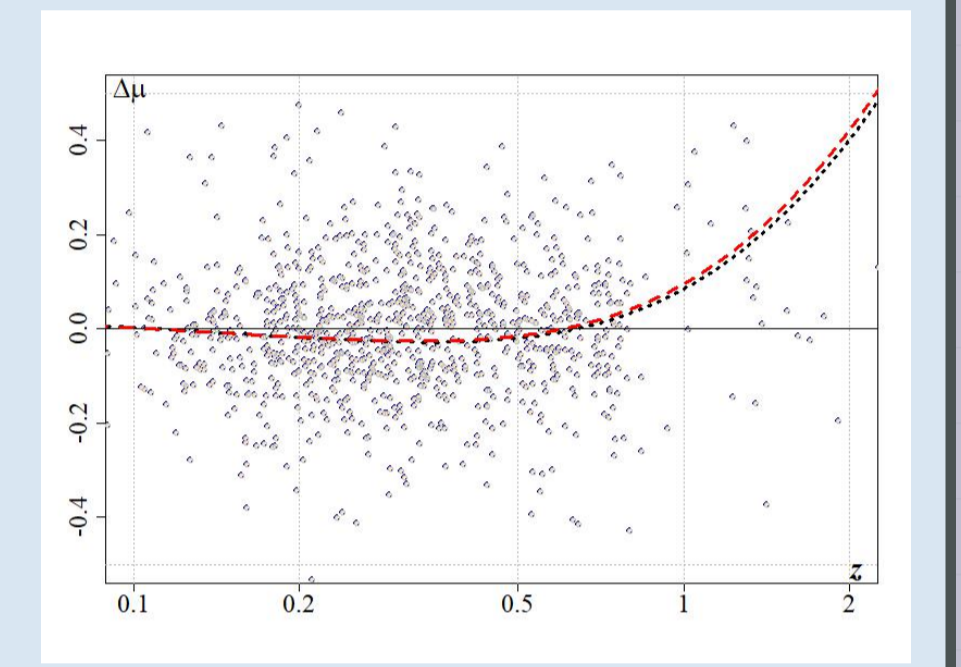
Fig.5: Distance moduli μ from the type Ia SNe "Pantheon+" sample (red points) as a function of redshift z , with the minimal χ^2 -fitted theoretical curves for the flat Λ CDM model (thin solid curve) and the ENdS model (dashed curve).



Fitting: ENdS

- In the case of ENdS, besides its free parameter r_o , the expression (1) requires an extra free parameter, such as s_g (a scaling factor), in order to match the theoretical μ_{ENdS} with the observationally determined μ from the type Ia SNe: $\mu_{\text{ENdS}} = 5 \log(s_g d_L) + 25$, because d_L is expressed in units of r_g , and we need to scale it to Mpc. Thus, the ENdS model, like the flat Λ CDM, also has two free parameters, the χ^2 -minimised values of which are $r_o - 1 = (9.91^{+0.02}_{-0.01}) \cdot 10^{-8}$; $s_g = (2.13^{+0.14}_{-0.13}) \cdot 10^{10}$ [Mpc], with the minimal $\chi^2_{\text{ENdS}} = 887.56$.

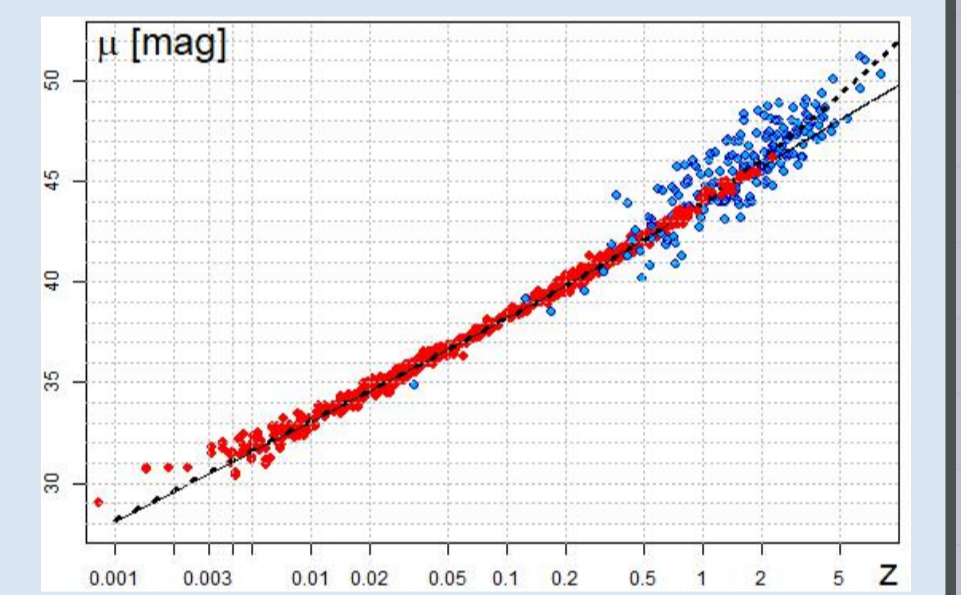
Fig.6: Differences $\Delta\mu$ [in stellar magnitude] between the Λ CDM fit to the 1701 type Ia supernova "Pantheon+" distance moduli (grey points) and the χ^2 -fitting of the cosmological model based on the ENdS space (dotted curve) to the same data. The latter curve is presented in the form of differences from the Λ CDM fit, which, thus, corresponds to the horizontal line at $\Delta\mu = 0$. The red dashed curve shows a slightly better fit of the ENdS-based model to the type Ia SN distance moduli when endowed with spacetime dynamics (similar to the FLRW scaling factor $a(t)$). This fit results in the minimised $\chi^2 = 886.39$ instead of 887.56 for the dotted curve.



Validation by GRB distance moduli

- Due to the lack of standard candle data for $z > 3$, we can get a hint of what these data might be by using a proxy to the standard candle data in the form of gamma-ray burst distance moduli μ_{GRB} obtained via the Amati relation [7]. As in Fig.5, the Λ CDM-based theoretical distance moduli are indicated by a thin solid curve, and the ENdS-based distance moduli are indicated by a thicker dashed curve.
- Without recalculating the model-parameter values obtained in the previous step, we have estimated the χ^2 using the combined GRB+SNe data as a validating data set for both models. The result of this validation is the following: $\chi^2_{\Lambda\text{CDM}} = 2104.8$; $\chi^2_{\text{ENdS}} = 2048.4$. The minimal χ^2 for the ENdS-based model is $\sim 2.7\%$ smaller than the minimal χ^2 for the Λ CDM model. This means that the static-universe model based on the ENdS space is a better predictor for high-redshifts observations than the expanding-universe Λ CDM model.

Fig.7: Distance moduli μ from the "Pantheon+" type Ia SNe sample (red points), together with the distance moduli from the GRB sample (blue points) calibrated using the Amati relation. The solid and dashed curves indicate the minimum χ^2 -fitted theoretical curves for the flat Λ CDM and ENdS models, respectively.



Conclusions

- The comparison between the standard Λ CDM cosmological model and the cosmological model proposed here demonstrates that these two models are practically identical in terms of their predictions for the distance moduli of the available standard candles (type Ia SNe) within the redshift range $0 < z < 2.3$.
- For higher redshifts, the model based on ENdS space predicts larger distance moduli (fainter type Ia SNe) than those calculated within the framework of the standard Λ CDM cosmological model. This theoretical prediction can be experimentally verified in the future, as new discoveries of type Ia SNe with $z \simeq 3$ are expected within a few years by the JWST.
- The 1998-discovery of type Ia SNe excessive dimming at $z \simeq 1$ was interpreted as evidence in favour of dark energy (repulsive gravity or the Λ -term in Einstein's equations). In physics, dark energy is an unknown entity, and it can only be viably physical interpreted in terms of vacuum energy. Experimental evidence from particle physics suggests that the vacuum energy density (due to quantum fluctuations) must be large enough that it is discrepant by the order of 10^{120} from what is currently deduced from type Ia SNe observations.
- In contrast, the competing model based on ENdS space discussed here exploits the experimentally observed effect of gravitational redshift. In addition, the ENdS model prediction can be appropriately validated in the near future via the expected aforementioned JWST discoveries.

References

- [1] de Sitter, W. On Einstein's theory of gravitation, and its astronomical consequences. Third paper, MNRAS 1917, 78, 3–28.
- [2] Einstein, A. Kosmologische betrachtungen zur allgemeinen Relativitätstheorie. Sitz. Preuss. Akad. Wiss. Phys. 1917, VL, 142–152.
- [3] Newcomb, S. Elementary theorems relating to the geometry of a space of three dimensions and of uniform positive curvature in the fourth dimension. J. für die reine und angewandte Mathematik 1877, LXXXIII, 293–299.
- [4] Scolnic, D., Brout, D., Carr, A., Riess, A.G., Davis, T.M., Dwomoh, A., Jones, D.O., Ali, N., Charvu, P., et al., The Pantheon+ Analysis: The Full Dataset and Light-Curve Release, ApJ 2022, 938, 113 (15pp).
- [5] Brout, D., Scolnic, D., Popovic, B., Riess, A.G., Zuntz, J., Kessler, R., Carr, A., Davis, T.M., et al., The Pantheon+ Analysis: Cosmological Constraints, ApJ 2022, 938, 110 (24pp).
- [6] Riess, A.G., Yuan, W., Macri, L.M., Scolnic, D., Brout, D., Casertano, S., Jones, D.O., Murakami, Y., et al., A comprehensive measurement of the local value of the Hubble constant with 1 km/s/Mpc uncertainty from the Hubble Space Telescope and the SHOES team, ApJL 2022, 934, L7 (52pp).
- [7] Amati, L., D'Agostino, R., Luongo, O., Muccino, M., Tantalò, M., Addressing the circularity problem in the $E_p - E_{\text{ISO}}$ correlation of gamma-ray bursts, MNRAS 2019, 486, L46–L51.